

Impact of Cation Concentration on Graphene Oxide Properties Fabricated from Disposed Batteries

Dong-Nghi Le¹, Tien-Luat Nguyen¹, Phuong V Pham², Tuan-Huu Nguyen¹, Thuy-Hong-Lam Ngo¹, Thien-Trang Nguyen¹, Van-Cuong Pham¹, Anh-Vu Phan-Gia¹, Huy-Binh Do^{1*}

¹Ho Chi Minh City University of Technology and Education, Vietnam

²National Sun Yat-sen University, Taiwan

*Corresponding author. Email: binhdh@hcmute.edu.vn

ARTICLE INFO

Received: 12/10/2023
Revised: 23/10/2023
Accepted: 23/10/2023
Published: 28/08/2024

KEYWORDS

Graphene;
Graphene oxide;
Electrochemical exfoliation;
Electrolyte solution;
Battery recycling.

ABSTRACT

Disposed batteries contain the hazardous sources that directly impact on the environment. Proper disposal of used batteries is a vital matter because of toxic component found in types of batteries. This study focuses on the reutilization of the disposed Zn-battery graphite to produce graphene oxide (GO) via electrochemical exfoliation. The influence of various electrolytes on the exfoliation process was investigated, and the optimal I_D/I_G values in Raman spectra were determined as 2.5% for KOH. Scanning electron microscopy (SEM) images confirmed the presence of multi-wall graphene oxide in the exfoliated samples. X-ray diffraction (XRD) spectra displayed a broadening of the peak at $2\theta = 26.5^\circ$, further supporting the successful formation of graphene oxide. The exfoliated graphene oxide was found not to contain any toxic elements. This highlights the potential of using disposed batteries in producing low cost graphene oxide. The study contributes to environmental protection by repurposing graphite rods and reducing industrial waste.

Doi: <https://doi.org/10.54644/jte.2024.1482>

Copyright © JTE. This is an open access article distributed under the terms and conditions of the [Creative Commons Attribution-NonCommercial 4.0 International License](https://creativecommons.org/licenses/by-nc/4.0/) which permits unrestricted use, distribution, and reproduction in any medium for non-commercial purpose, provided the original work is properly cited.

1. Introduction

In recent years, there has been a notable increase in battery consumption due to the arrival of the technological age. As a consequence, used batteries have become a hazardous form of waste, directly impacting the environment. Proper disposal of these batteries has become an urgent matter due to the unique chemical components found in each type [1]. Notably, graphite rods within Zinc-carbon batteries can serve as potential sources for recycling graphite. Therefore, the recycling of graphite rods from disposed batteries is crucial, aiming to reuse graphite in batteries, reduce pollution, and enable the production of graphene oxide (GO). Graphene oxide was initially synthesized through the process of oxidizing and exfoliating naturally crystalline graphite [2]. GO has 2D structure as graphene, however, layers of carbon are covalently bonded to oxygen-containing groups such as hydroxyl, epoxide, carbonyl, etc [3]. These functional groups are present both on the basal plane and at the edges, and they are introduced during the chemical exfoliation process of graphite flakes. The presence of these functional groups in GO enables easy processing and provides it with high colloidal stability in water, giving rise to a distinctive range of mechanical, colloidal, and optical properties [4]. The properties of GO can be enhanced using chemical engineering techniques, resulting in a wide range of applications such as solar cells [5], sensors [6], supercapacitors [7], cellular migration [8], drug delivery [9], membranes [10], multifunctional gels [11], water purification [12].

Electrochemical exfoliation [13] is a promising method to produce graphene and graphene oxide due to its possibility of the mass-production. In this method, the ions of electrolyte intercalate between the graphene layers, exfoliating them to single layer or few layers. Numerous electrolytes and electrochemical conditions have been tested with excellent exfoliation efficiencies. Applied voltage and the type of electrolyte strongly affect the quality of graphene oxide, especially in the presence of negative ions such as SO_4^{2-} , NO_3^- , Cl^- , etc [14], [15]. Using high voltage during the exfoliation also generates numerous oxygen groups on exfoliated graphene oxide and damages its structure [16]. To address this

issue, researchers have explored the use of negative potentials under cathodic conditions in the presence of positive intercalation ions like tetraalkylammonium cations. This approach aims to prevent the formation of oxygen functionalities and achieve higher-quality graphene [16]. However, it has been observed that the exfoliation efficiencies under cathodic conditions are generally lower compared to anodic conditions.

In this study, graphene oxide is fabricated using the electrochemical exfoliation of graphite rods obtained from disposed Zin-batteries. Because the cation concentration strongly affects the exfoliation efficiencies, the initial investigation of KOH concentration of 2.5% and 7.5% was conducted to see the impacts of the cation concentration on the properties of GO. The GO fabricated was thoroughly analyzed in terms of its morphology, structure, and crystalline properties, using scanning electron microscopy (SEM), Raman spectroscopy, and X-Ray diffraction analysis (XRD).

2. Experimental Procedure

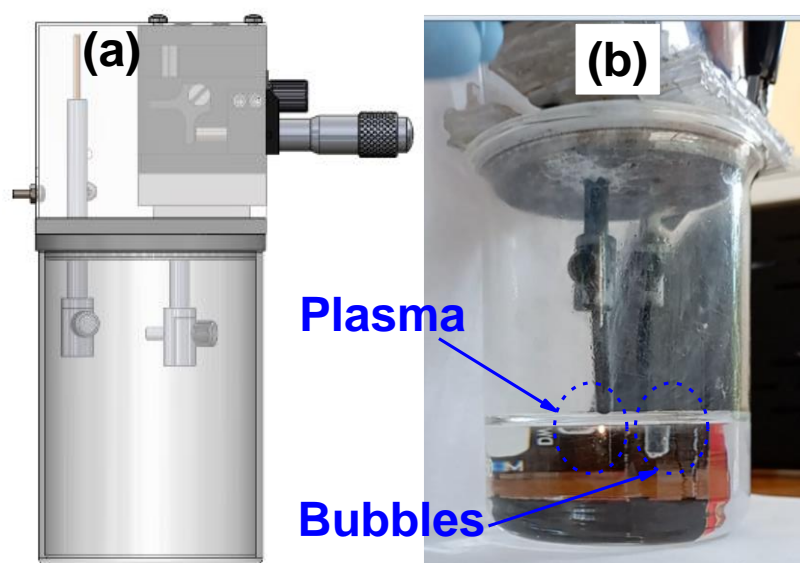


Figure 1. (a) The electrochemical cell was illustrated schematically, clearly indicating the placement of the cathode and anode. Notably, the cathode was designed to be movable along a perpendicular axis with respect to the bottom of the chamber. (b) Observations revealed that plasma generation occurred specifically at the cathode, while bubbles were observed exclusively at the anode within the electrolyte solution.

The electrolytic solution used in this study was created by dissolving KOH in 200 ml of water and $(\text{NH}_4)_2\text{SO}_4$ in 40 ml of water. The KOH and $(\text{NH}_4)_2\text{SO}_4$ solutions were prepared individually, then combined and stirred for 10 minutes. The anode and cathode were obtained from graphite rods with a diameter of 6 mm (Pinaco, the eagle brand). The tip of the cathode was ground to approximately 200 μm in diameter. Prior to the experiment, all electrodes underwent a cleaning process using acetone and isopropanol (IPA), followed by annealing at 130°C for 24 hours. The experimental setup involved an electrochemical chamber, as showed in Figure 1(a), where a specially designed cap allowed for unrestricted movement of the cathode. To begin the experiment, all electrodes were linked to a DC power supply, and the bias voltage was gradually raised up to 60 V. The initial temperature inside the chamber was noted as 30°C. In order to induce graphene exfoliation, the cathode was slowly lowered in increments of 20 μm until a plasma formed around its tip (as shown in Figure 1(a)). At this moment, numerous bubbles were emitted at the anode, and a gas was expelled from the chamber as illustrated in Figure 1(b). Throughout the experiment, graphene oxide (GO) underwent exfoliation, causing it to float on the surface of the electrolyte solution. The plasma state was sustained for over one hour. Subsequently, the GO was washed with deionized (DI) water and gathered by employing vacuum filtration through a Poly(vinylidene fluoride) (PVDF) membrane with an average pore size of 0.45 μm . The sample was then subjected to a drying process at a temperature of 50°C for a duration of 2 hours.

Hitachi FE-SEM S-4800 was utilized to obtain scanning electron microscope (SEM) images. The Raman spectra were obtained using the Horiba XploRA ONE system.

3. Results and Discussion

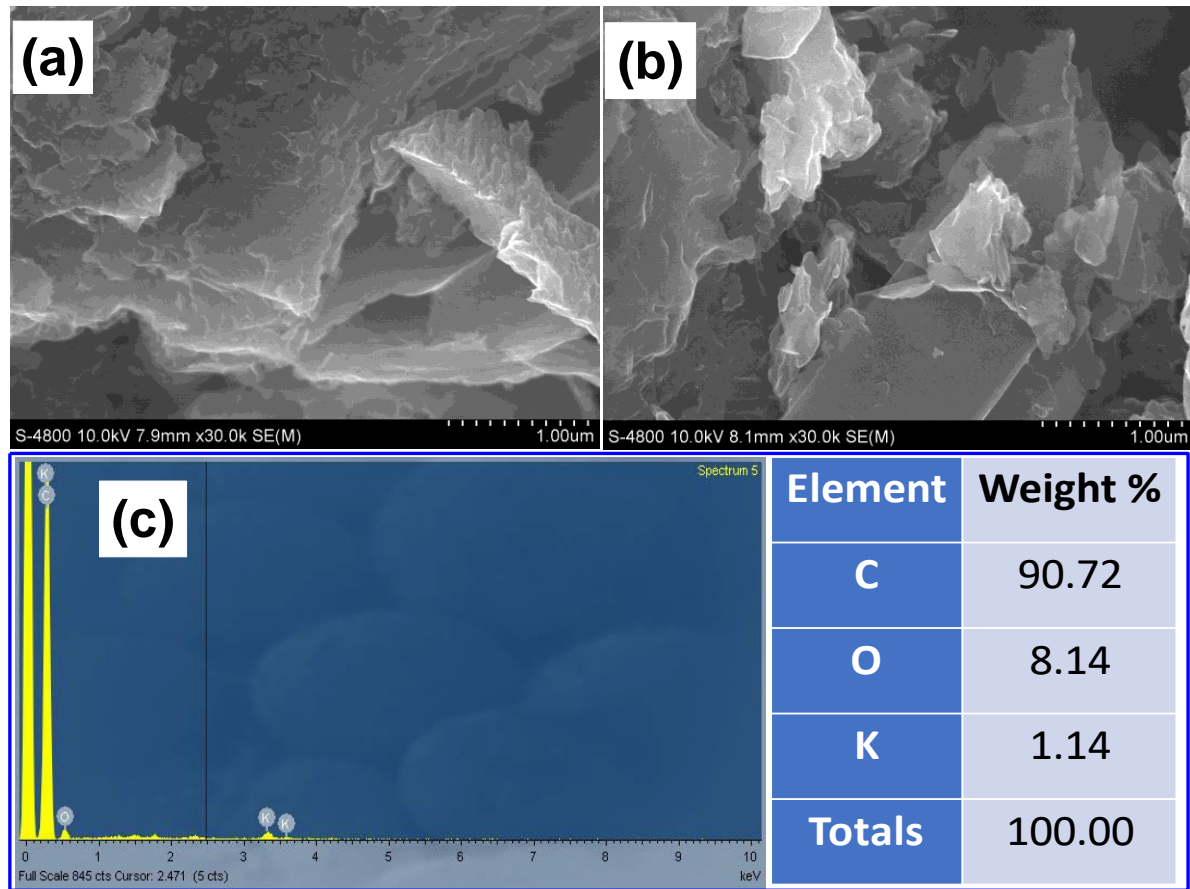


Figure 2. The scanning electron microscope (SEM) images depict (a) graphite and (b) graphene oxide (GO) obtained using the plasma-assisted exfoliation method with 2.5%. In Figure 2(a), a stacked layer structure and bulk form of graphite are observed. Conversely, Figure 2(b) displays crumpled nanosheets resulting from the exfoliation process. Notably, Figure 2(b) illustrates the scrolled configuration of GO. Figure 2(c) presents the Energy-Dispersive X-ray Spectroscopy (EDS) spectrum of GO after the filtration process. The analysis reveals that no toxic metals are detected in the samples.

Fig. 2 displays electron microscope images obtained from a field emission scanning electron microscope (FESEM). The images compare graphite powder, which was directly obtained by grinding a graphite rod, with exfoliated graphene oxide collected after filtration. In Fig. 2(a), the graphite powder exhibits a stacked layer structure, indicating the presence of multiple layers. On the other hand, Fig. 2(b) shows the result of plasma-assisted electrochemical exfoliation, where randomly crumpled nano-sheets are formed. The closely associated nano-sheets in the exfoliated product are a result of the strong π - π bonds between them. These nano-sheets form nanometer-scale plates, composing the exfoliated product. Notably, upon observation, the graphene oxide (GO) sheets can be seen to be scrolled, as indicated in the inset of Fig. 2(b). Figure 2(c) presents an investigation of the purification of exfoliated graphene oxide (GO) through an Energy-Dispersive X-ray (EDX) spectrum analysis. The analysis aimed to identify any toxic elements present in GO. Upon examination, it was determined that no toxic elements were detected. A small fraction of potassium (K) was observed within the marginal errors of the EDX measurement. This finding suggests that GO can be utilized for various applications without concerns regarding toxic heavy metal content.

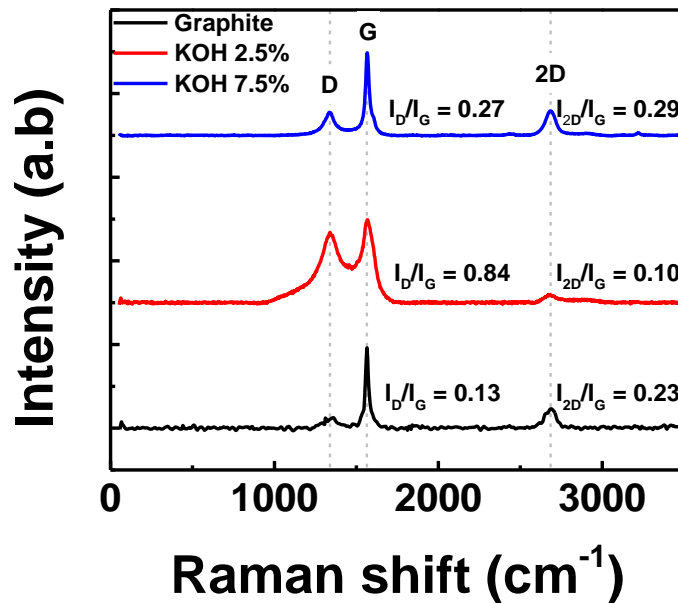
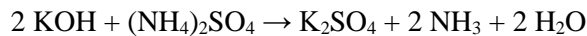


Figure 3. The Raman spectra of graphite powder (black line) and graphene oxide (red and blue lines) reveal clear distinctions. Specifically, when the KOH concentration is 2.5%, the spectrum of graphene oxide shows broadening and shifting of peaks towards higher frequencies. This shift is indicative of isolated double bonds present in the single layer of graphene oxide.

The influence of cations on the reduction of defects at the surface and edge of GO has been reported [16], even though exfoliation is facilitated by anions like SO_4^{4-} , NO_3^{3-} , Cl^- . Figure 3 illustrates the Raman spectra analysis exploring the effects of varying potassium concentrations on the properties of GO. In the electrolyte solution, the reaction between KOH and $(\text{NH}_4)_2\text{SO}_4$ can be represented by the following chemical equation:



In this reaction, potassium hydroxide (KOH) reacts with ammonium sulfate $(\text{NH}_4)_2\text{SO}_4$ to form potassium sulfate (K_2SO_4), ammonia (NH_3), and water (H_2O). The presence of K^+ and SO_4^{4-} ions in the solution can be inferred from this observation. Raman spectra of graphite and GO in Fig. 3 illustrates structural changes during the chemical conversion from graphite to graphene oxide. It is well-known that C=C bonds exhibit high Raman intensities [17]. In the case of graphite spectra (represented by the black line), the peak with the highest intensity occurs at 1568.8 cm^{-1} , corresponding to its G bands. This peak results from the first-order scattering of the E_{2g} phonon of sp^2 carbon atoms [18]. The G band is observed in all sp^2 carbon materials, including graphite, amorphous carbon, carbon nanotubes, and graphene. Additional weak bands are associated with the D band at 1342.3 cm^{-1} and the 2D band at 2682.3 cm^{-1} . The D band is known as a defect band and arises from edge effects, structural defects, and the breaking of symmetry in sp^2 bonds. The presence of the 2D peak in the Raman spectra of graphene oxide is attributed to the linear dispersion of its electronic bands, resulting in either triple resonance or double resonance. It is important to note that the Raman spectra of graphene oxide are influenced not only by the phonon properties but also by its electronic structures.

In 2.5% KOH sample, the frequencies of the D band, G band, and 2D band experienced a shift towards higher values in this study. Specifically, the D band reached a value of 1348.45 cm^{-1} , the G band reached 1572.42 cm^{-1} , and the 2D band reached 2678.98 cm^{-1} . These findings align with previous reports [19], [20]. During the exfoliation process of graphite to graphene oxide, there are notable changes observed in the G and D bands. These changes can be seen in Fig. 3 as a broadening and rightward shift of these bands (red line). The rightward shift of the G band suggests a higher resonance frequency associated with isolated double bonds present in single layer graphene oxide [21]. Additionally, an increase in the I_D/I_G ratio from 0.13 (representing graphite, depicted by the black line) to 0.81 (representing graphene oxide, shown by the red line) in Fig. 3 indicates a decrease in the size and crystallinity of graphitic materials. This increase in the ratio signifies the presence of more isolated

graphene domains [18], [19]. These observations align with findings reported in [20]. When the concentration of KOH is increased to 7.5%, a noticeable shift in the frequencies of the D band, G band, and 2D band is also observed. This shift is opposite to that observed in the 2.5% KOH sample (represented by the blue line). In this sample, the D band frequency is measured at 1339.93 cm^{-1} , the G band frequency at 1567.66 cm^{-1} , and the 2D band frequency at 2683.91 cm^{-1} . The shift in these bands indicates that the high concentration of K^+ cations has a suppressive effect on the defects present on the surface and edges of the graphene. However, this higher concentration may result in a lower efficiency of exfoliation. This can be attributed to the strong bonds formed between the K^+ cations and SO^{4-} anions, which minimize the interlacement of SO^{4-} ions between the graphene sheets.

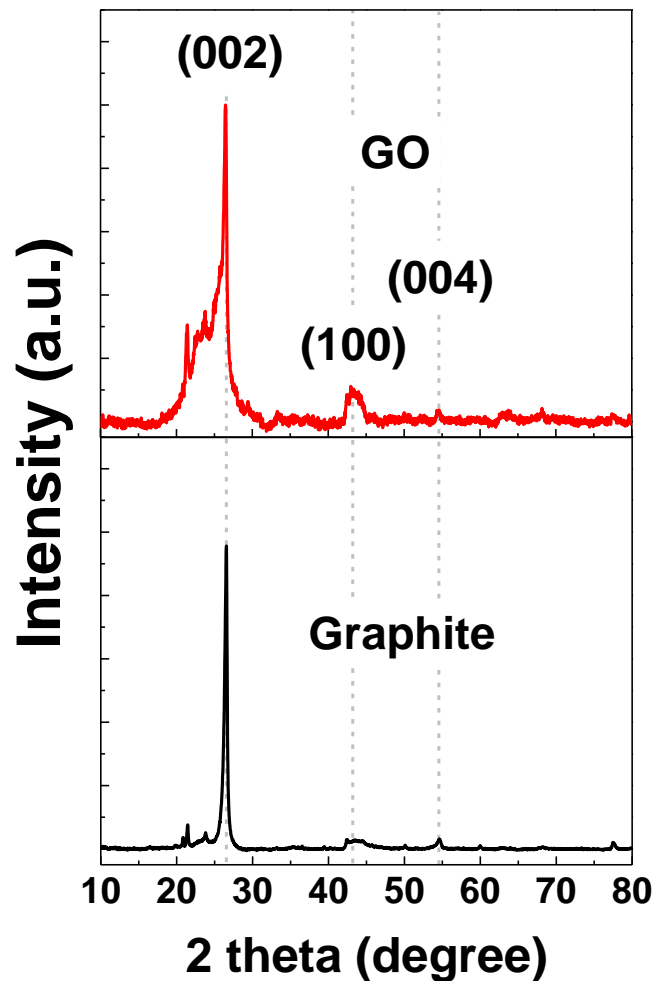


Figure 4. XRD patterns recorded for graphite and graphene oxide obtained from plasma-assisted exfoliation.

The graphite-based material (GF) was analyzed using X-ray diffraction (XRD) in Fig. 4 (black line). A distinct diffraction peak at $2\theta = 26.54^\circ$ was observed, exhibiting a narrow peak width and high intensity. This peak corresponds to the crystal plane (002) of graphite, which possesses a hexagonal structure and an interlayer distance of $d = 0.34\text{ nm}$ [22]. Additionally, a peak with small intensity at $2\theta = 54.5^\circ$ was detected, corresponding to the crystal plane (004). The (004) peak is weaker as compared to the (002) peak because it is a result of a second-order diffraction [23]. The XRD pattern of the GO sample shows a significant shift and expansion towards lower angles. This broad peak locates from $2\theta = 20.53^\circ$ to approximately $2\theta = 26.65^\circ$, indicating an expanded interlayer distance ranging between 0.33 nm and 0.43 nm. These changes indicate that the graphite is exfoliated to GO during electrochemical exfoliation process. Additionally, a lower intensity peak at $2\theta = 42.60^\circ$ ($d = 0.21\text{ nm}$) is observed, corresponding to the (100) peak. This peak can be attributed to the presence of disorder in carbon materials [24], [25]. The appearance of (100) peak is a result of the oxidation of SO^{4-} ions during the exfoliation process at the anode.

4. Conclusions

In conclusion, graphene oxide (GO) was successfully synthesized from disposed zinc batteries. The focus was on investigating the influence of potassium concentration on the properties of GO. Raman spectra analysis revealed that the presence of cation K^+ effectively reduced defects on the graphene surface and its edges, presenting a promising approach to improve the quality of fabricated graphene oxide. X-ray diffraction (XRD) spectra demonstrated a broadening of the (002) peak of carbon, indicating the successful exfoliation of graphite layers to form graphene oxide. The confirmation of obtained GO was further supported by scanning electron microscopy (SEM) and energy-dispersive X-ray spectroscopy (EDS) analysis. Importantly, no toxic elements were detected in the exfoliated GO, emphasizing the potential of this study in producing cost-effective GO while contributing to environmental protection through the repurposing of discarded batteries.

Acknowledgments

This work was funded by the Ho Chi Minh City University of Technology and Education, Vietnam (Grant No. SV2023-43).

Conflict of Interest

The authors declare no conflict of interest.

REFERENCES

- [1] D. Acuti, L. Lemarié, and G. Viglia, "How to enhance the sustainable disposal of harmful products," *Technological Forecasting and Social Change*, vol. 186, p. 122151, 2023.
- [2] A. Hussain, Y. Weng, and Y. Huang, "Graphene and Graphene-Based Nanomaterials: Current Applications and Future Perspectives," *Drug Delivery Using Nanomaterials*, pp. 209-228, 2022.
- [3] S. Lin *et al.*, "Tuning oxygen-containing functional groups of graphene for supercapacitors with high stability," *Nanoscale Advances*, vol. 5, pp. 1163-1171, 2023.
- [4] R. Kumar and R. Thangappan, "Electrode material based on reduced graphene oxide (rGO)/transition metal oxide composites for supercapacitor applications: a review," *Emergent Materials*, vol. 5, pp. 1881-1897, 2022.
- [5] M. Kladaew, J. Y. Lin, N. Chanlek, V. Vailikhit, and P. Hasin, "Well-Dispersive Polypyrrole and MoSe₂ Embedded in Multiwalled Carbon Nanotube@Reduced Graphene Oxide Nanoribbon Electrocatalysts as the Efficient Counter Electrodes in Rigid and Plastic Dye-Sensitized Solar Cells," *ACS Applied Energy Materials*, vol. 6, pp. 397-415, 2023.
- [6] R. A. Campos, K. Eersels, R. Rogosic, T. J. Cleij, H. Diliën, and B. van Grinsven, "Imprinted Polydimethylsiloxane-Graphene Oxide Composite Receptor for the Biomimetic Thermal Sensing of *Escherichia coli*," *ACS Sensors*, vol. 7, pp. 1467-1475, 2022.
- [7] B. Singh, R. Kaur, R. Kaur, K. Singh, and S. Rana, "A highly stable solid-state supercapacitor device based on robust layer-by-layer electrodeposited poly-(3, 4-ethylenedioxythiophene)-reduced graphene oxide-molybdenum disulfide nanocomposite electrode," *Journal of Energy Storage*, vol. 56, p. 105926, 2022.
- [8] S. Sun *et al.*, "Graphene oxide-based plasma membrane-philic delivery platform to generate tolerogenic dendritic cells in GVHD immunotherapy," *Nano Today*, vol. 46, p. 101578, 2022.
- [9] A. Shafiee, S. Iravani, and R. S. Varma, "Graphene and graphene oxide with anticancer applications: Challenges and future perspectives," *MedComm*, vol. 3, p. e118, 2022.
- [10] J. Ye, C. Zheng, J. Liu, T. Sun, S. Yu, and H. Li, "In Situ Grown Tungsten Trioxide Nanoparticles on Graphene Oxide Nanosheet to Regulate Ion Selectivity of Membrane for High Performance Vanadium Redox Flow Battery," *Advanced Functional Materials*, vol. 32, p. 2109427, 2022.
- [11] Y. Yan *et al.*, "Robust and Multifunctional 3D Graphene-Based Aerogels Reinforced by Hydroxyapatite Nanowires for Highly Efficient Organic Solvent Adsorption and Fluoride Removal," *ACS Applied Materials & Interfaces*, vol. 14, pp. 25385-25396, 2022.
- [12] H. Qu *et al.*, "Graphene Oxide Nanofiltration Membrane Based on Three-Dimensional Size-Controllable Metal-Organic Frameworks for Water Treatment," *ACS Applied Nano Materials*, vol. 5, pp. 5196-5207, 2022.
- [13] Y. Lei, B. D. Ososon, P. L. Trahan, J. Chen, J. Perreault, and A. C. Tavares, "Electrochemically Exfoliated Graphene Oxide for Simple Fabrication of Cocaine Aptasensors," *ACS Applied Materials & Interfaces*, vol. 15, pp. 35580-35589, 2023.
- [14] J. Yang *et al.*, "Trace-H₂O₂ Boosting the Reaction Kinetics of H₂SO₄ Intercalation into Graphite for the High-Oxidation Efficiency Preparation of Graphene Oxide for Na Ion Storage," *ACS Applied Nano Materials*, vol. 6, pp. 14810-14819, 2023.
- [15] Q. Yu *et al.*, "Electrochemical synthesis of graphene oxide from graphite flakes exfoliated at room temperature," *Applied Surface Science*, vol. 598, p. 153788, 2022.
- [16] W. W. Liu and A. Aziz, "Review on the Effects of Electrochemical Exfoliation Parameters on the Yield of Graphene Oxide," *ACS Omega*, vol. 7, pp. 33719-33731, 2022.
- [17] B. Paulchamy, G. Arthi, and B. Lignesh, "A simple approach to stepwise synthesis of graphene oxide nanomaterial," *J Nanomed Nanotechnol*, vol. 6, p. 1, 2015.
- [18] N. A. Kumar, H. J. Choi, Y. R. Shin, D. W. Chang, L. Dai, and J. B. Baek, "Polyaniline-grafted reduced graphene oxide for efficient electrochemical supercapacitors," *ACS nano*, vol. 6, pp. 1715-1723, 2012.
- [19] C. Fu, G. Zhao, H. Zhang, and S. Li, "Evaluation and characterization of reduced graphene oxide nanosheets as anode materials for lithium-ion batteries," *Int. J. Electrochem. Sci*, vol. 8, pp. 6269-6280, 2013.
- [20] M. Bera, P. Gupta, and P. K. Maji, "Facile one-pot synthesis of graphene oxide by sonication assisted mechanochemical approach and its surface chemistry," *Journal of nanoscience and nanotechnology*, vol. 18, pp. 902-912, 2018.
- [21] S. Stankovich *et al.*, "Synthesis of graphene-based nanosheets via chemical reduction of exfoliated graphite oxide," *carbon*, vol. 45, pp. 1558-1565, 2007.

- [22] M. Salverda, A. R. Thiruppathi, F. Pakravan, P. C. Wood, and A. Chen, "Electrochemical exfoliation of graphite to graphene-based nanomaterials," *Molecules*, vol. 27, p. 8643, 2022.
- [23] N. Cao and Y. Zhang, "Study of reduced graphene oxide preparation by Hummers' method and related characterization," *Journal of Nanomaterials*, vol. 2015, pp. 2-2, 2015.
- [24] N. Sazali *et al.*, "Preparation and structural characterization of turbostratic-carbon/graphene derived from amylose film," in *AIP Conference Proceedings*, 2016.
- [25] V. Thirumal, A. Pandurangan, R. Jayavel, and R. Ilangoan, "Synthesis and characterization of boron doped graphene nanosheets for supercapacitor applications," *Synthetic Metals*, vol. 220, pp. 524-532, 2016.



Le Dong Nghi is currently an undergraduate student in the Department of Materials Technology, Faculty of Applied Science, HCMC University of Technology and Education. Email: 19130035@student.hcmute.edu.vn. ORCID: <https://orcid.org/0009-0007-1053-649X>



Nguyen Tien Luat is currently an undergraduate student in the Department of Materials Technology, Faculty of Applied Science, HCMC University of Technology and Education. Email: 19130031@student.hcmute.edu.vn. ORCID: <https://orcid.org/0009-0004-7797-6607>



Pham V Phuong is currently an assistant professor in the Department of Physics, National Sun Yat-sen University (NSYSU), Taiwan. He is a pioneering scientist in materials science and electronics/optoelectronics. He has participated in industrial projects with Samsung, POSCO, the Government of Korea, the Ministry of Education and the Ministry of Science and Technology of China, and the National Science and Technology Council (NSTC), Taiwan. Email: phuongpham@mail.nsysu.edu.tw. ORCID: <https://orcid.org/0000-0001-7951-1329>



Nguyen Tuan Huu is currently an undergraduate student in the Department of Materials Technology, Faculty of Applied Science, HCMC University of Technology and Education. Email: 20130032@student.hcmute.edu.vn. ORCID: <https://orcid.org/0009-0008-7123-8856>



Ngo Thuy Hong Lam is currently an undergraduate student in the Department of Materials Technology, Faculty of Applied Science, HCMC University of Technology and Education. Email: 20130041@student.hcmute.edu.vn.




Nguyen Thien Trang was an undergraduate student in the Department of Materials Technology, Faculty of Applied Science, HCMC University of Technology and Education. Email: 18130046@student.hcmute.edu.vn.




Pham Van Cuong was an undergraduate student in the Department of Materials Technology, Faculty of Applied Science, HCMC University of Technology and Education. Email: Cuongvt116@gmail.com.



Phan Gia Anh Vu is currently a senior lecturer, and the dean of Faculty of Applied Science, HCMC University of Technology and Education. Email: yuphan@hcmute.edu.vn. ORCID:  <https://orcid.org/0009-0008-7412-5232>



Do Huy Binh received the Ph.D. degree from the National Chiao Tung University, Taiwan. He is currently a lecturer in the Department of Materials Technology, Faculty of Applied Science, HCMC University of Technology and Education. Email: binhdh@hcmute.edu.vn. ORCID:  <https://orcid.org/0000-0003-3274-5050>